PAPER Nr. : 32

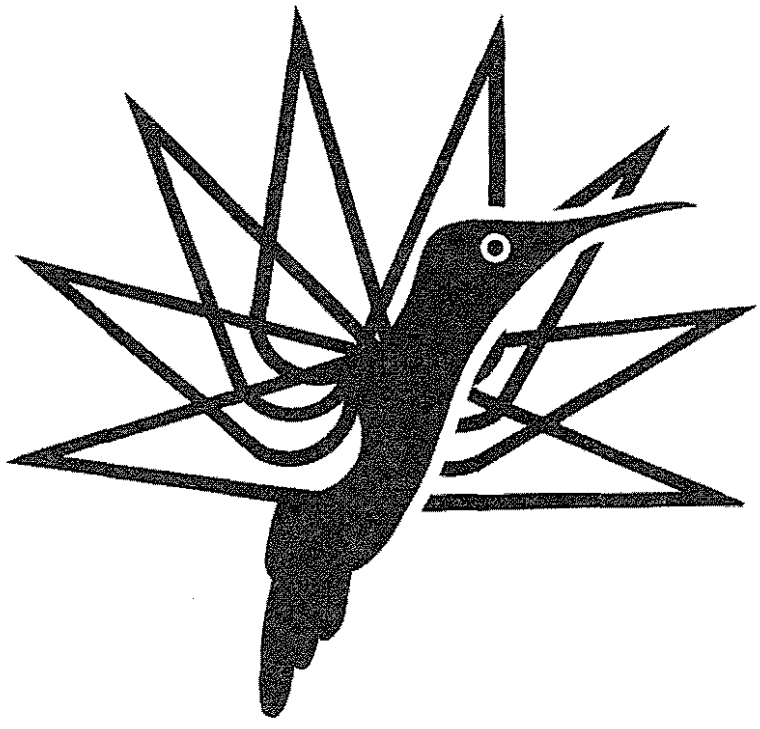

EFFECT OF CHANGING ROTOR PARAMETERS ON ROTOR WAKE VELOCITIES AT VERY LOW ADVANCE RATIOS

by

Henry R. Velkoff, Professor
Hanan Terkel, Research Assistant
Fu Kuo Shaio, Research Assistant

The Department of Mechanical Engineering
The Ohio State University
Columbus, Ohio U.S.A.

FIFTH EUROPEAN ROTORCRAFT AND POWERED LIFT AIRCRAFT FORUM
SEPTEMBER 4 – 7TH 1979 - AMSTERDAM, THE NETHERLANDS

LIST OF SYMBOLS

b	Number of blades, dimensionless
c	Blade chord, inch
i	Shaft angle, degrees
I_B	Flapping Moment of Inertia, slugs - feet^2
k^2	Constant to express the deviation from Cosine-Law of cylindrical anemometer sensors, dimensionless
V_{eff}	Effective cooling velocity of a sensor, feet/second
V	Magnitude of velocity vector, feet/second
X	Wind tunnel coordinate direction
Y	Wind tunnel coordinate direction
Z	Wind tunnel coordinate direction
μ	Advance ratio, dimensionless
Θ	Collective angle, degree
δ	Angle between direction of V and cylindrical sensor

ABSTRACT

Tests were conducted on a two bladed teetering model helicopter rotor and on a two bleded rotor with twisted blades at very low advance ratios. Data on the time-average structure of the rotor wake were taken using a three wire hot-film probe. The findings present data which may be useful in further understanding the nature of the wake at low speed flight of helicopters and may prove useful in the development of models for the rotor wake.

EFFECT OF CHANGING ROTOR PARAMETERS ON ROTOR WAKE VELOCITIES AT VERY LOW ADVANCE RATIOS

H. R. Velkoff, H. Terkel, F. Shaio
The Ohio State University
Columbus, Ohio U.S.A.

1. INTRODUCTION

The need for data or helicopter rotor wakes at low advance ratios has increased because the recent emphasis on low speed nap-of-the earth flight. To provide data for this region of flight, tests using a model rotor in a wind tunnel have been conducted. The initial data obtained utilized a two bladed model rotor at advance ratios of 0.04 through 0.10 and were reported in a recent paper (1). In those initial tests data were provided at only one value pitch angle, $\Theta = 8°$, and shaft tilt, $i = 8°$. The results of those initial tests revealed that the overall rotor flow tended to roll-up into two descreet vortices similar to a low aspect ration wing. A particularly unique flow characteristic was also observed at the advance ratios of $\mu = 0.08$ and below. This characteristic was the pronounced tendency for the flow to not only form the two vortices, but to also present concentrated regions of inhanced magnitude of the axial component of velocity in the vortex. Such localized regions of high dynamic pressure associated with the vortices could possibly affect the design of empenage for helicopters.

Since data in the low advance ratio region are limited, primarily that of reference 1, Heyson and Katsoff (2), and Bowden and Shockey (3), further tests were planned and undertaken to secure a wider range of data. The data presented here includes tests of a two bladed rotor at a given pitch angle and three tilt angles. A twisted blade rotor was also tested to evaluate the effect of blade twist on rotor wake velocity.

2. EXPERIMENTAL ARRANGEMENT

The tests were conducted in a wind tunnel with a 8 foot by 4 foot test section. The flow turbulence is reduced by means of a 2 to 1 contraction ratio, nested 1/8 inch diameter straws, and three layers of screening. The tunnel with the turbulence reduction system in place provides air velocities up to 75 feet per second. Further details on the wind tunnel can be found in reference 4.

3. ROTOR CHARACTERISTICS

The rotors which were tested are indicated below.

Two Bladed Rotor

Teetering Rotor

Rotor radius	1.25, feet
Blade chord	2.125, inch
Rotor solidity	$bc/\pi R = 0.0902$
Root cutout	%R = 11.7
Blade taper ratio	= 1
Coning angle	= 0°
Blade aspect ratio	$\frac{r}{c} = 7.06$
Blade twist	= 0°
Airfoil section NACA	0012
I_B	= 0.005583 slug-feet^2

Two Bladed Rotor With Twisted Blades

Teetering Rotor

Rotor radius	1.25, feet
Blade chord	2.1875, inch
Rotor solidity	$bc/\pi R = 0.0928$
Root cutout	%R = 12.08
Blade taper ratio	= 1
Coning angle	= 0°
Blade twist	= 8° (From 12.08%R to 100%R)
Airfoil section NACA	0012
I_B	= 0.004260 slug-feet^2

The rotors are driven by a variable speed electric motor. The collective pitch and the shaft angle are adjustable. The rotors are not trimmed but are allowed to flap freely. There is no rotor moment developed in either of the rotors tested. Figure 1 illustrates the general location of the rotor in the cross section of the wind tunnel.

4. FLOW MEASUREMENT

The velocity data obtained are time average data taken with a three-dimensional hot-film probe connected to three DISA 55D05/102C constant temperature anemometer circuits. Details of the hot wire circuitry used and the method of data reduction may be found in reference 1. In summary each hot film probe is calibrated for

the effects of changes in direction. Of specific importance to obtaining data at low tunnel speeds associated with low advance ratios is the fact that the hot-films must operate at very low probe Reynolds numbers. At such conditions the value of k^2 in the directional correction equation

$$Veff^2/V^2 = \sin^2\delta + k^2 \cos^2\delta$$

can vary significantly. Variation in k^2 can lead to errors in the computed spatial angles of the velocity vectors. In these tests calibration of the effect of low Reynolds number on k^2 was accomplished. A typical result for a TSI 1294-60-18 0.006" diameter hot-film probe is shown in Figure 2.

5. TRAVERSE MECHANISM

The hot-film probe was positioned at discreet points throughout the region of the rotor wake, both below and above the rotor. The region traversed was from 0.4 radius above the rotor to 0.8 radius below the rotor, laterally out to 1.2 radius, and 28 inches forward of the rotor centerline and 40 inches aft of the rotor center. The data points were located at 3 inches along rotor axis, 4 inches laterally and 4 inches along the tunnel centerline or tunnel flow direction. A total of 1584 measurement-locations result. However the number of points is reduced since data can not be taken in the vicinity of the rotor plane. Further details on the traversing system may be found in reference 1.

6. ERROR ANALYSIS

An extensive discussion of the errors in velocity and angle measurements and probe location is also presented in reference 1. In general the error in angular measurement is believed to be of the order of 2°, velocity in the order of $\pm$ 1 feet per second, tunnel speed of the order of 2%, rotor speed to within 2%, and probe position to within $\pm$ 0.25 inches.

7. TEST RESULTS

The test conditions for the two bladed teetering rotor were

Blade tip speed, feet/second	300
Advance ratio	0.06
Collective pitch angle, degrees	8
Rotor shaft tilt, degrees	2,4,8
Coning angle, degrees	0

An additional test was run for a two bladed teetering rotor with twisted blades. The test conditions for this rotor were

Blade tip speed, feet/second	300
Advance ratio	0.06
Collective pitch angle at 75%R, degrees	8
Twist angle, (From 12.08%R to 100%R) degrees	8
Rotor shaft tilt, degrees	8
Coning angle, degrees	0

The data are presented in terms of computer generated vector plots. Components of the total velocity, V, are shown in X-Y, Y-Z, and Z-X planes. The locations of these planes (X-Y, Y-Z, etc.) is depicted in Figure 3. It should be remembered that the data presented are average velocity data, averaged at each point over many revolutions of the rotor, and that the rotors are not trimmed, and do not generate rotor moment.

Data are presented for advance ratio of 0.06, pitch angle of 8 degrees, and shaft angles of 2, 4, 8 degrees. For the shaft angle of 8 degrees, an additional condition is presented with twisted blades. For the last case the twist is two degree for the blade's length and the pitch angle was measured at 75% of the radius.

Figure 4 presents the data for $i = 8°$ for the transverse Y-Z plane. The expected rollup as the flow moves downstream can be observed from the data. Figure 5 for $i = 8°$, depicts the various longitudinal X-Z planes showing the downwash influence of the rotor. Figure 6 for $i = 8°$ and X-Y planes show the flow field when viewed from "above" the rotor and the lateral flow due to rollup can be seen.

For $i = 4°$ Figure 7 presents the transverse Y-Z planes, Figure 8 presents the longitudinal X-Z planes and Figure 9 presents the X-Y planes.

For $i = 2°$ Figure 10 presents the transverse Y-Z planes, Figure 11 presents the longitudinal X-Z planes and Figure 12 presents the X-Y planes.

Figure 13 presents the transverse Y-Z planes for $i = 8°$ and twisted blades. Figure 14 presents the longitudinal X-Z planes and Figure 15 presents the X-Y planes.

8. DISCUSSION OF TEST RESULTS

Examination of the data for $\mu = 0.06$ was shown in the Y-Z planes in Figures 4, 7, 10, 13 reveals a vortex rollup similar to what would be expected behind a low aspect ratio wing. In this particular case the intensity of the vortex developing aft of the advancing side (on the right hand side of the figure) seems to be

greater than the vortex developed aft of the retreating side. Figures 4, 7, 10 which depict shaft angles of 8, 4, 2 respectively. do not show a distinct change in the flow pattern, and one would have to use a more thorough statistical analysis to interpret the influence of shaft angle on the rotor's wake. Figure 13 reveals that the vortex intensity is much greater for the twisted blades but the general shape of two vortices rolling up remains the same.

The flow pattern when viewed from the side of the rotor (X-Z planes) Figures 5, 8, 11, 14 shows an anticipated up flow in the plane outside the rotor tip on the advancing side (Y/R = 1.33). Just inside the rotor tip at Y/R = -0.8 a strong downwash pattern develops. Closer to the hub at Y/R = -0.267 the downwash pattern is still evident. At Y/R = 0.0 the downwash pattern is still apparent but reduced in intensity. At the retreating side at Y/R = 0.53 a highly concentrated region of downwash is again evident. The flow beyond the tip at Y/R = 1.33 is upwards similar to the plane at Y/R = -1.33. As with the Y-Z planes, changes in shaft angle do not reveal a significant alteration in the flow pattern (Figures 5, 8, 11). However, the twisted blade creates a larger longitudinal component (X direction) as well as a stronger downwash (Z direction).

The "squirt effect" discussed in reference (1) is revealed in these experiments again. The X-Z planes for the twisted blades at Y/R = -0.267 and Y/R = -0.533 are actually revealing a funnel like behaviour. The flow coming out of the rotor between X/R = -0.8 and X/R = -1.07 is squirted aft is concentrated streams.

The view from above the rotor, Figures 6, 9, 12, 15 reveals the anticipated inflows above the trailing vortex structure, Z/R = 0.2. At Z/R = 0.0 and below the rotor one can see the outflow in the region of the trailing vortex. For these planes, again the change in shaft angle does not show a significant effect on the flow pattern, but the rotor with the twisted blades creates a more distinct flow pattern by having bigger velocity components in the x and y directons.

9. ACKNOWLEDGEMENT

Specific mention must be made for the valuable help of several undergraduate students whose willingness to work long and unusual hours contributed to the success of the data acquisition. They are: R. Cooley, K. Yamarak, R. Cooke, R. Navarro, and T. Parker.

REFERENCES

1. H. R. Velkoff, and D. Horak, Rotor Wake Measurements At Very Low Advance Ratios, 35th Annual Forum of the American Helicopter Society, Paper Nr. 79-6, Washington, D.C., May 1979.

2. H. H. Heyson, and S. Katzoff, Induced Velocities Near A Lifting Rotor With Nonuniform Disc Loading, NASA Rep. 1319, 1957.

3. T. H. Bowden, and G. A. Shockey, A Wind Tunnel Investigation Of The Aerodynamic Environment Of A Full-Scale Helicopter Rotor In Forward Flight, Bell Helicopter Company, USAAVLABS Technical Report 70-35, U. S. Army Aviation Material Laboratories, Fort Eustis, Virginia, July 1970.

4. H. R. Velkoff, D. A. Blaser, and K. M. Jones, Boundary Layer Discontinuity On A Helicopter Rotor Blade In Hovering, AIAA Journal of Aircraft, Vol. 8, No. 2, 1971.

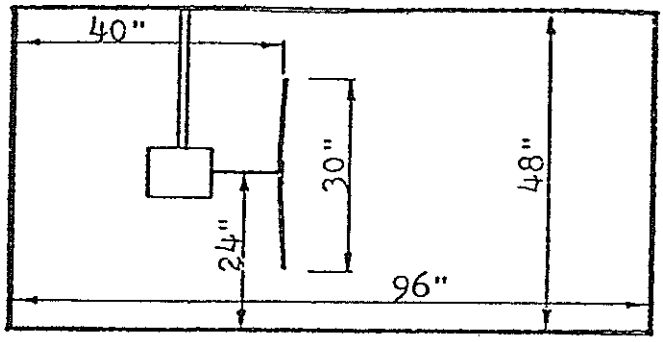

FIGURE 1. Location of the Rotor in the Test Section.

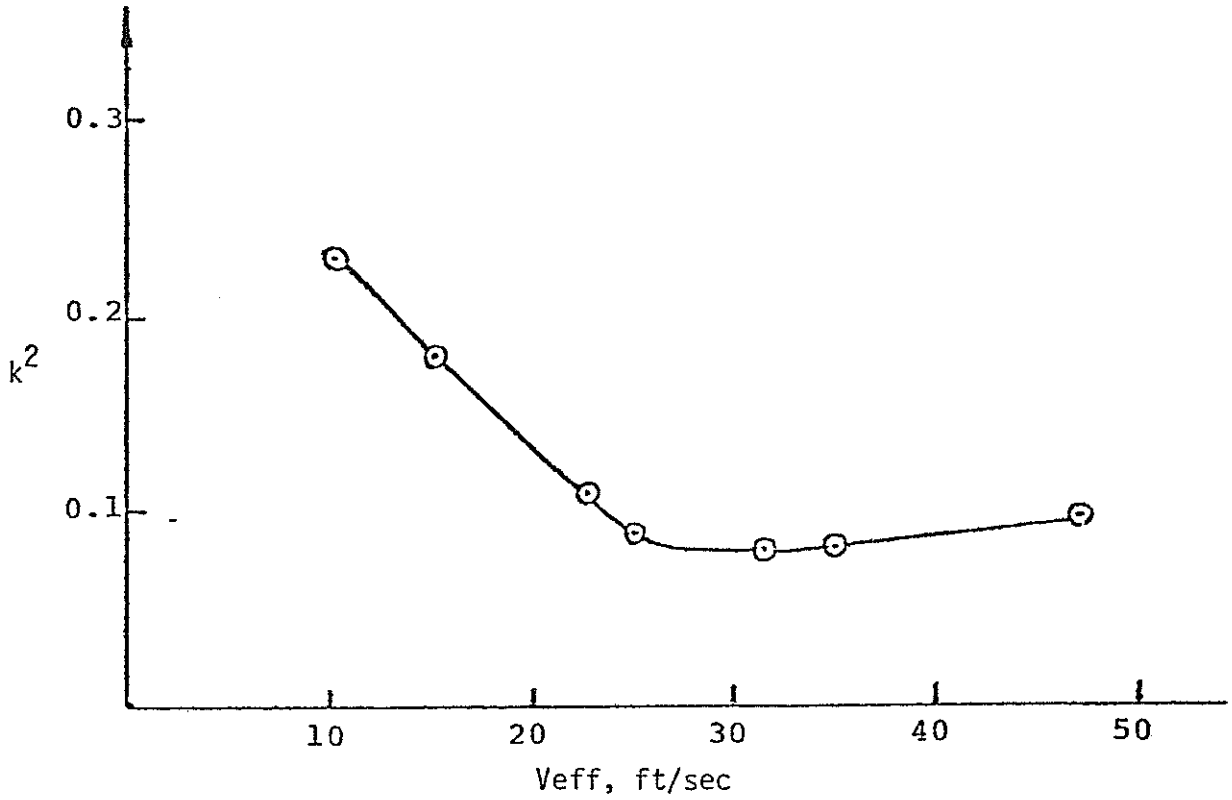

FIGURE 2. Changes of k^2 as a Function of Veff

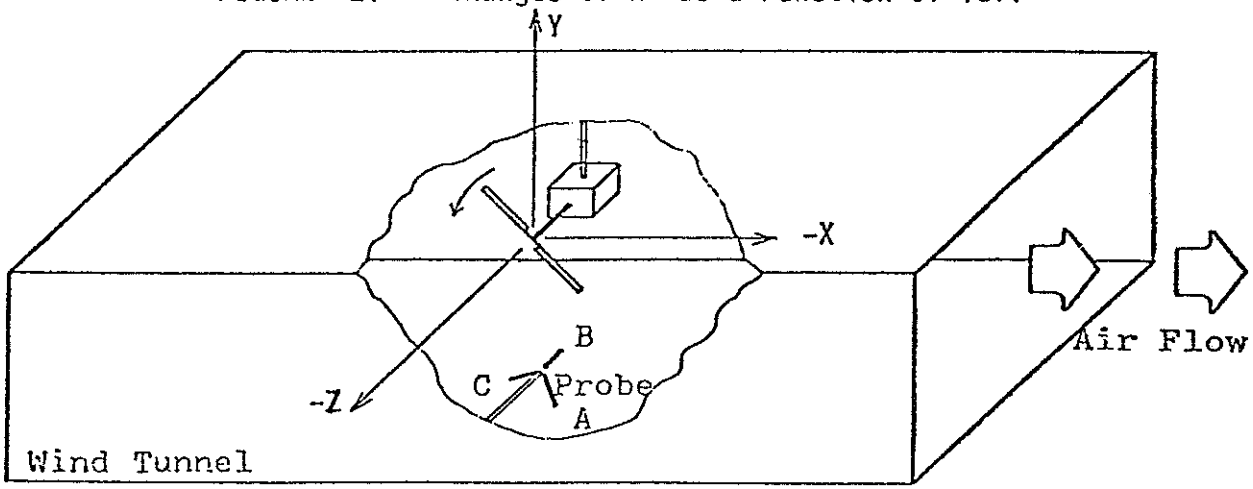

FIGURE 3. The Spatial Orientation of the Hot Film inthe Wind Tunnel.

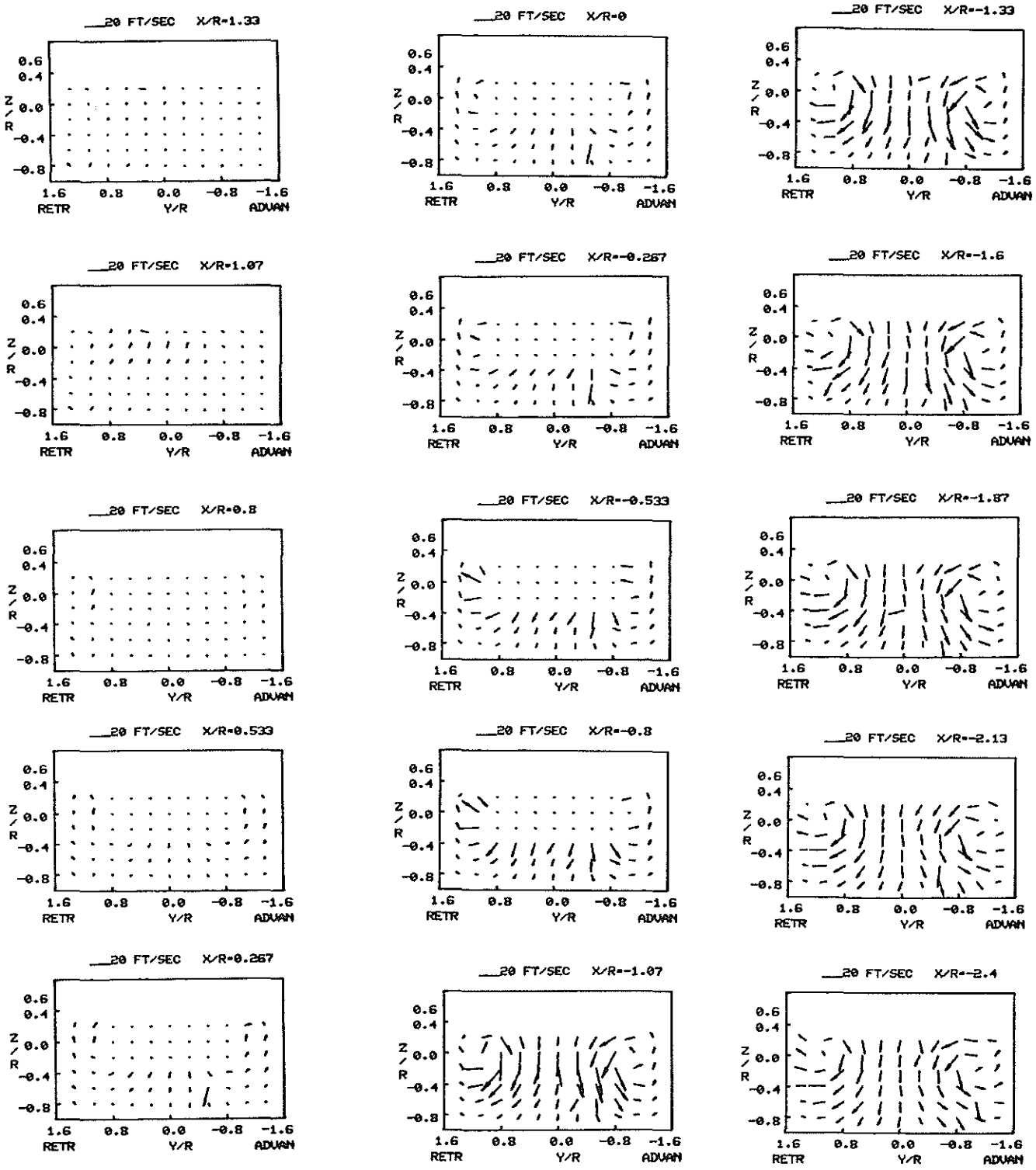

Figure 4.

Velocity vectors in Y-Z plane for μ=0.06, θ=8°, and i=8°. Note that coordinates depict probe position only.

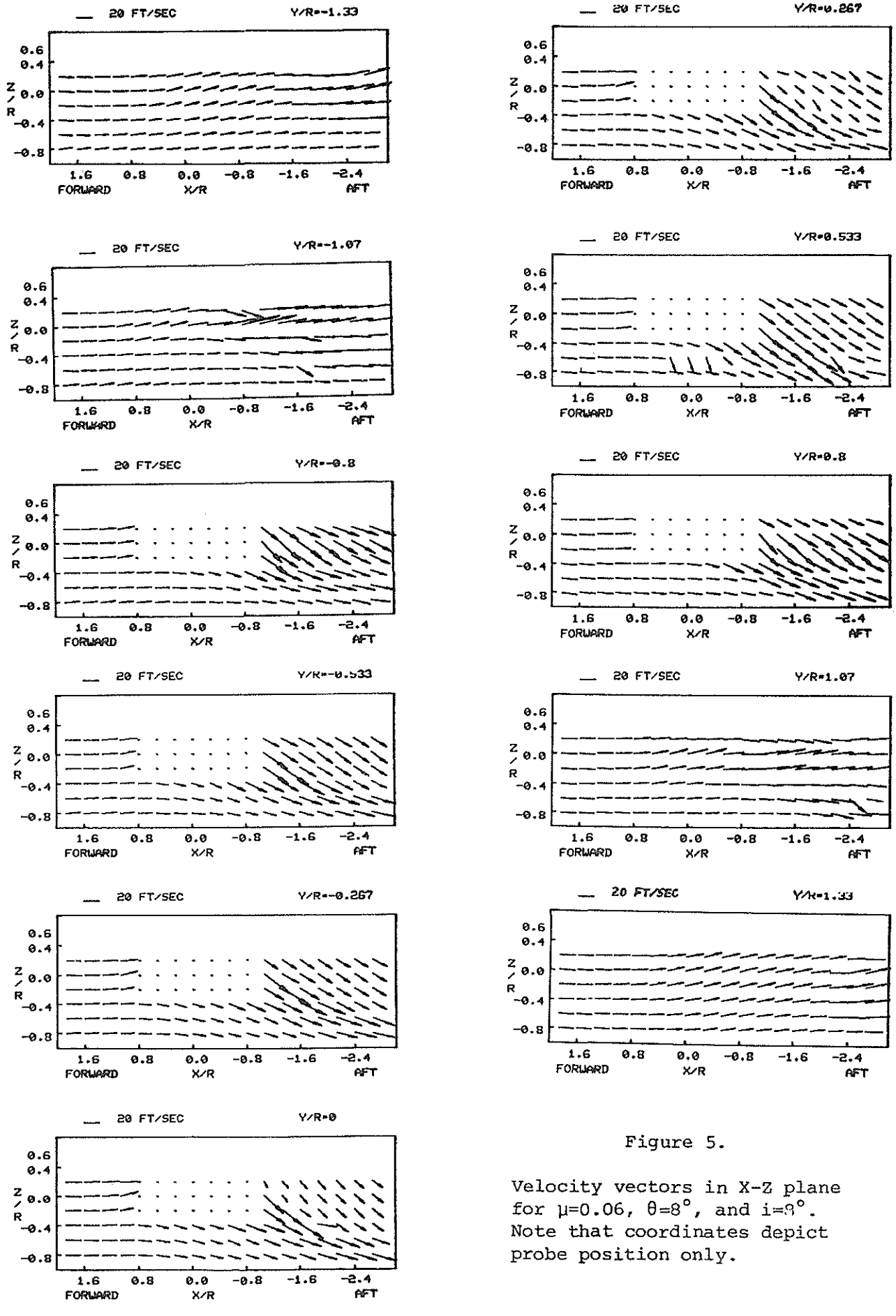

Figure 5.

Velocity vectors in X-Z plane for μ=0.06, θ=8°, and i=9°. Note that coordinates depict probe position only.

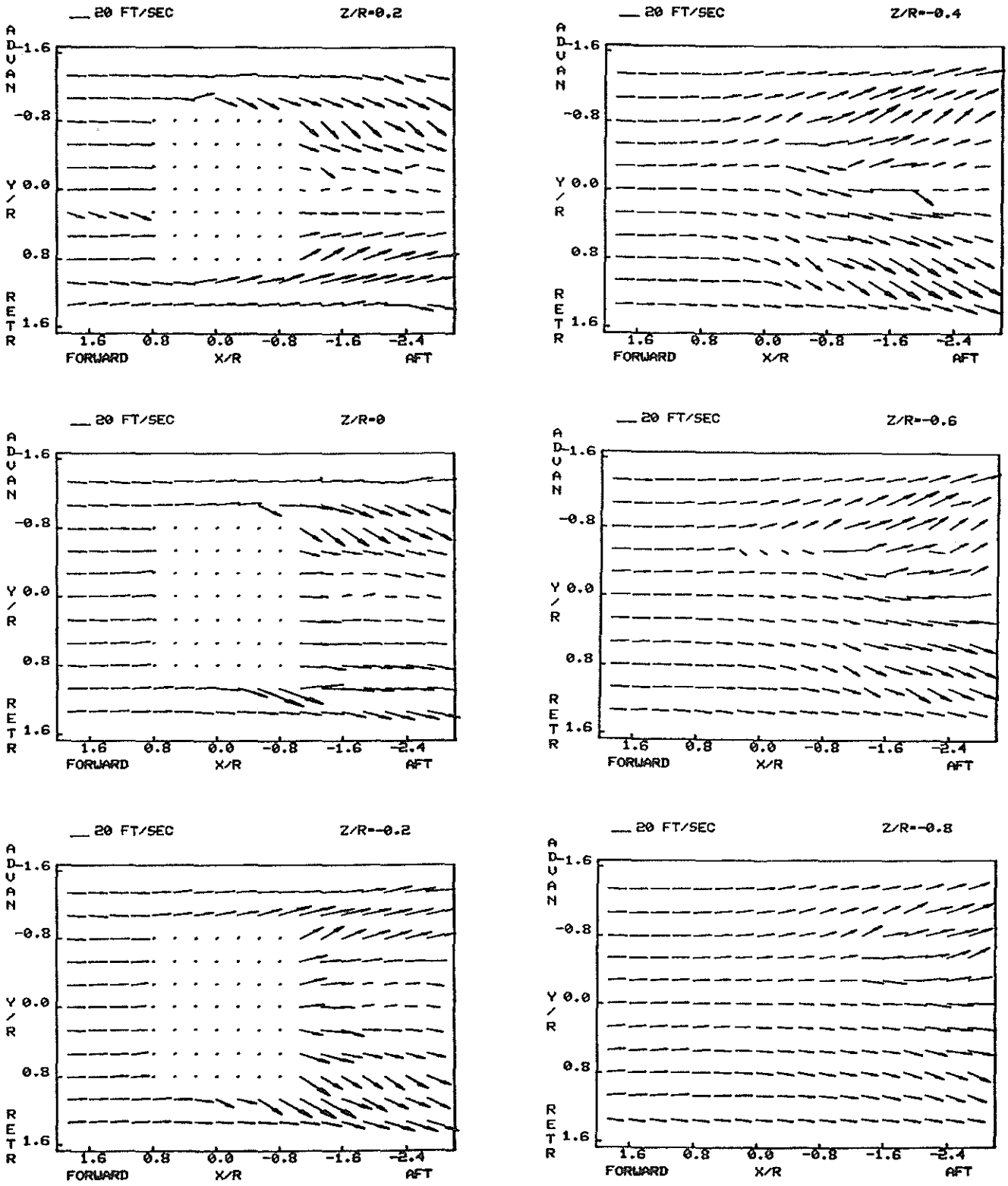

Figure 6.

Velocity vectors in X-Y plane for μ=0.06, θ=8°, and i=8°. Note that coordinates depict probe position only.

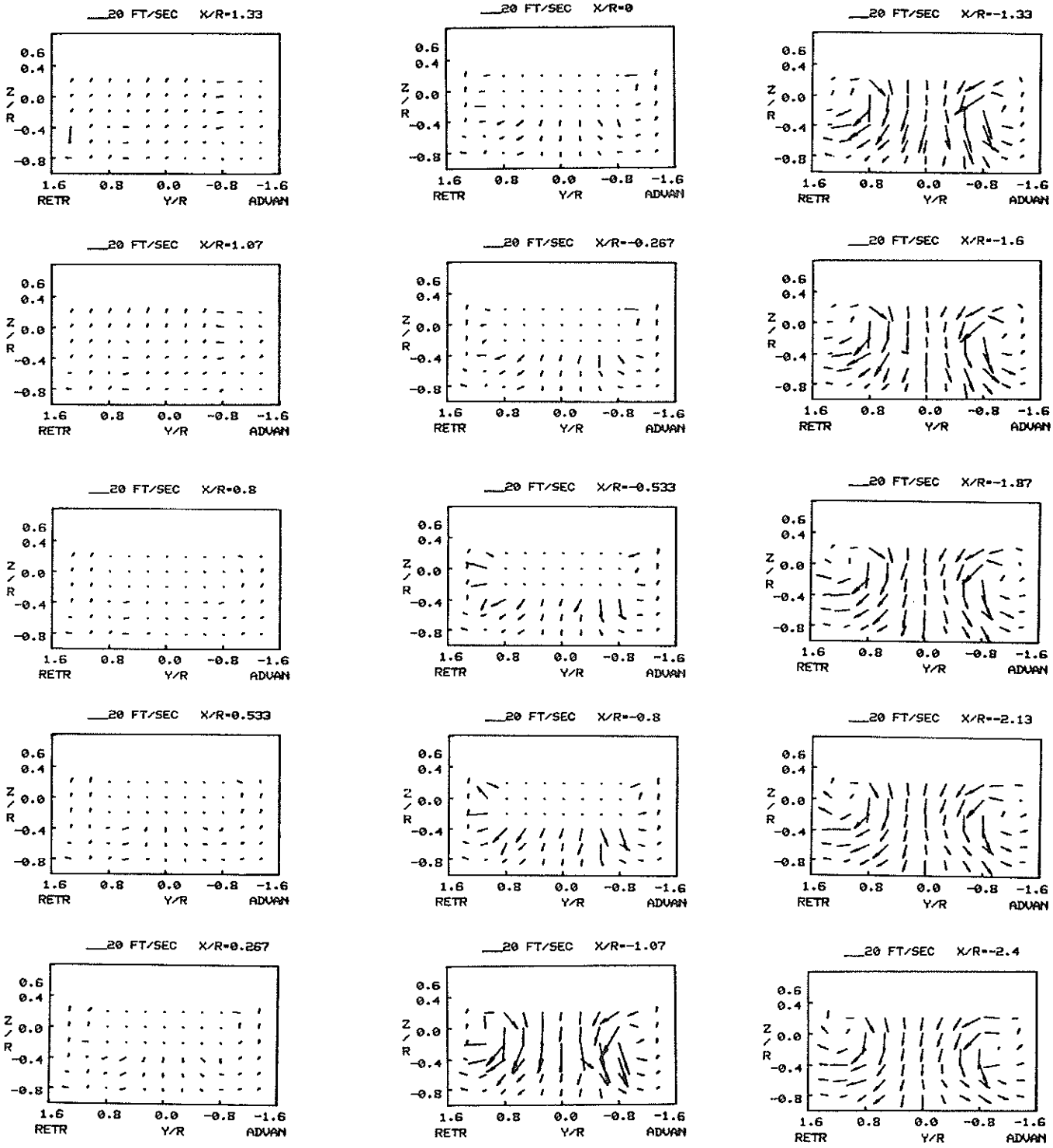

Figure 7.

Velocity vectors in Y-Z plane for μ=0.06, θ=8°, and i=4°. Note that coordinates depict probe position only.

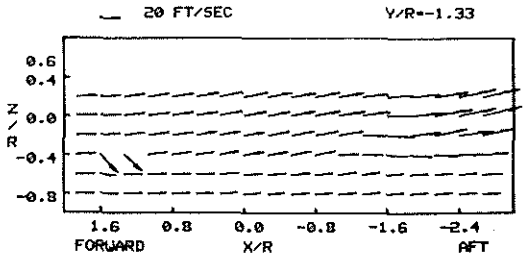

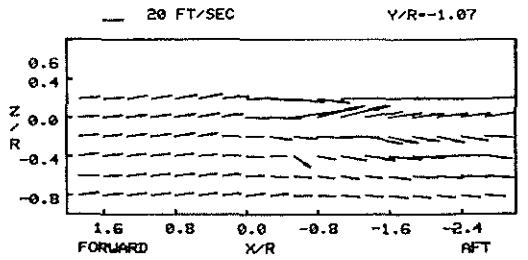

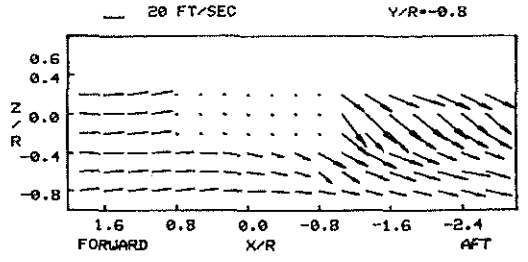

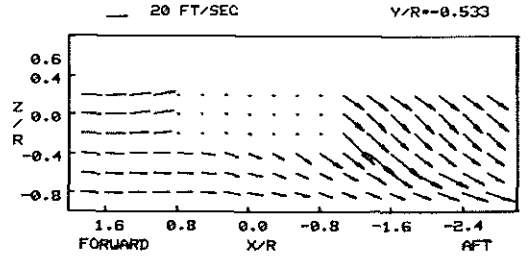

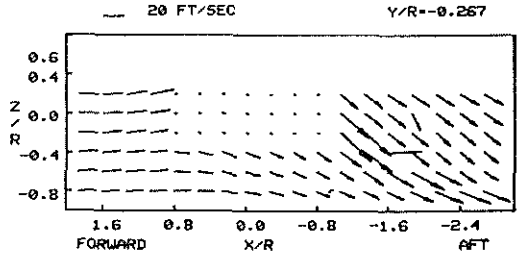

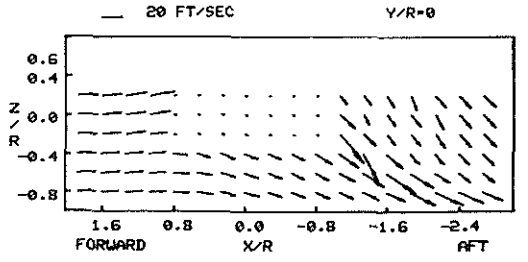

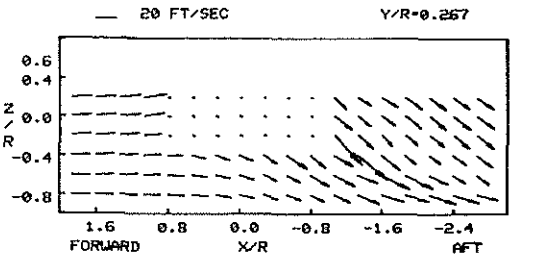

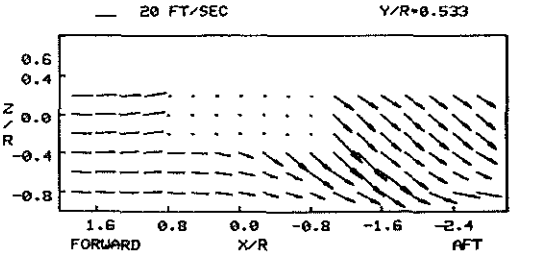

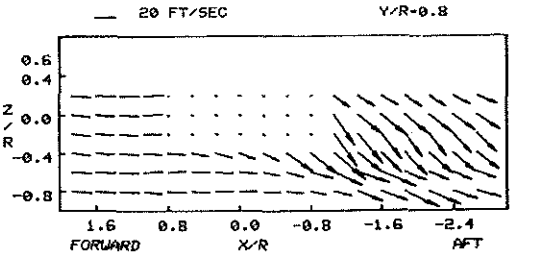

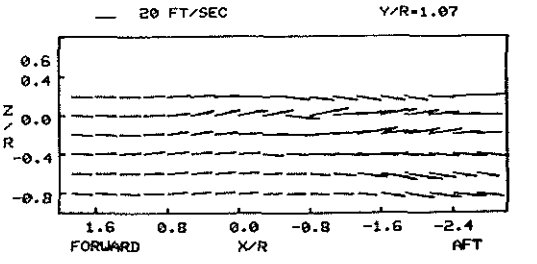

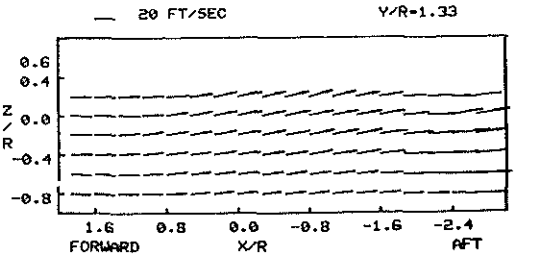

Figure 8.

Velocity vectors in X-Z plane for μ=0.06, θ=8°, and i=4°. Note that coordinates depict probe position only.

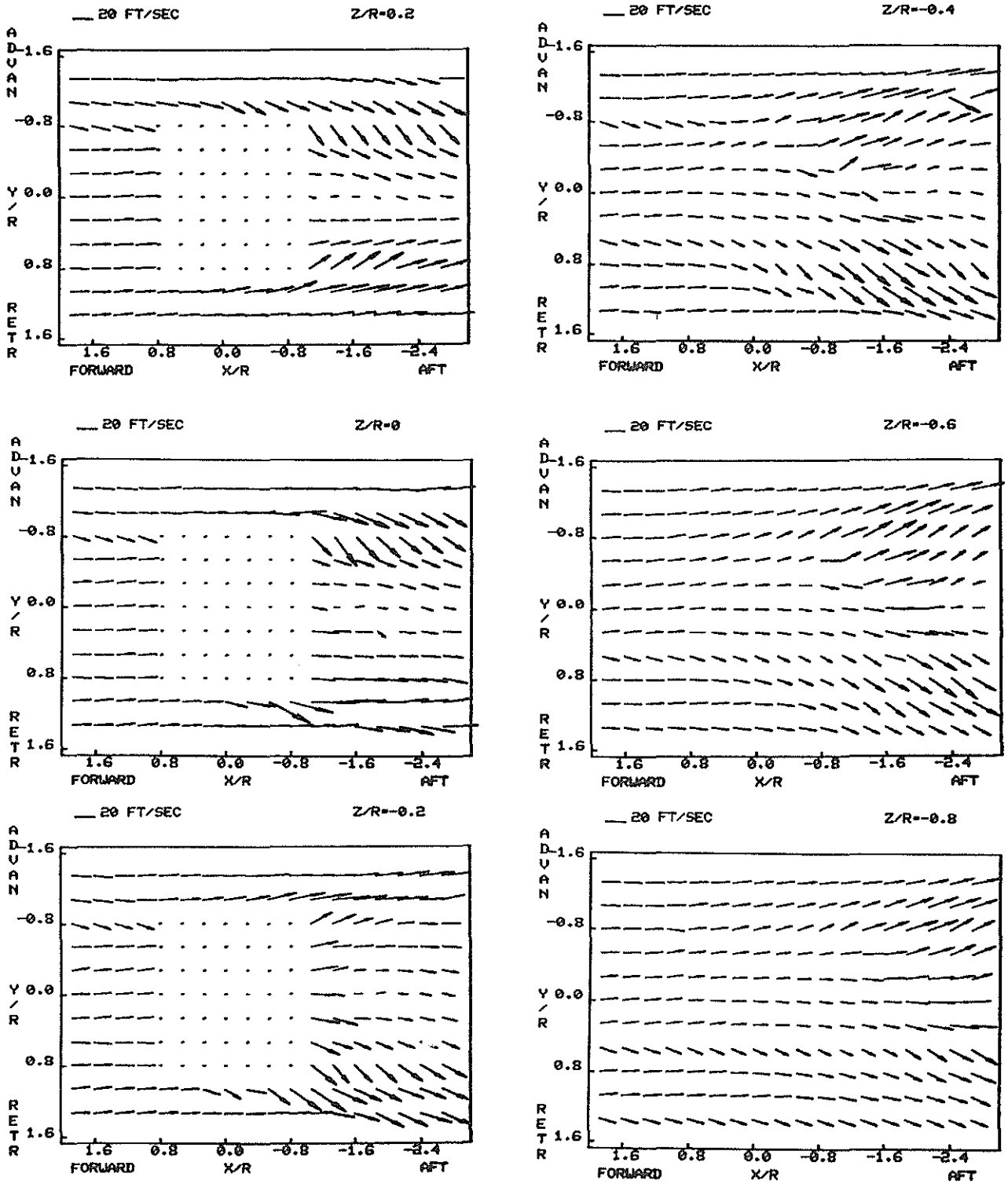

Figure 9.

Velocity vectors in X-Y plane for μ=0.06, θ=8°, and i=4°. Note that coordinates depict probe position only.

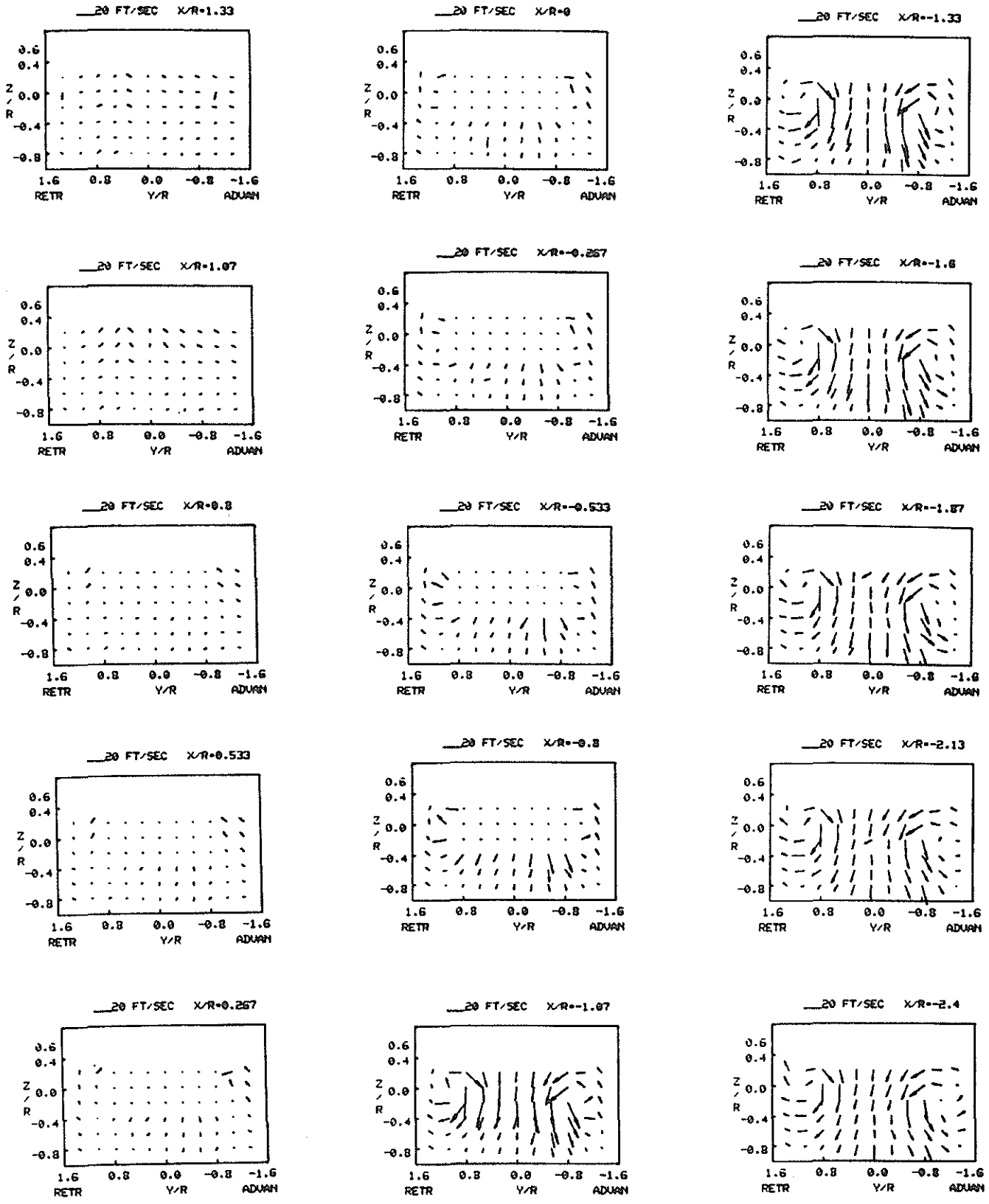

Figure 10.

Velocity vectors in Y-Z plane for μ=0.06, θ=8°, and i=2°. Note that coordinates depict probe position only.

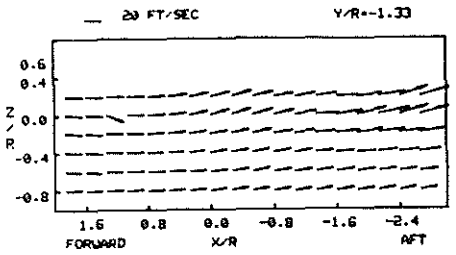

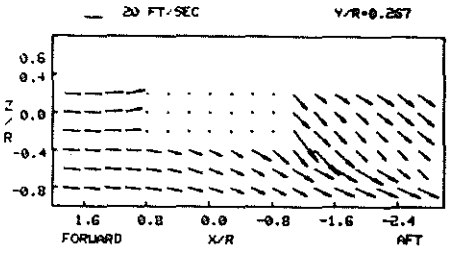

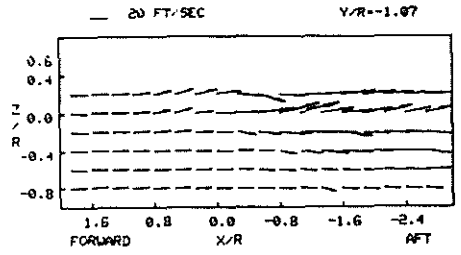

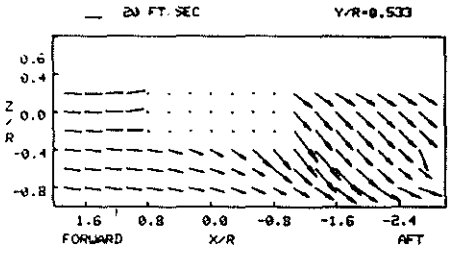

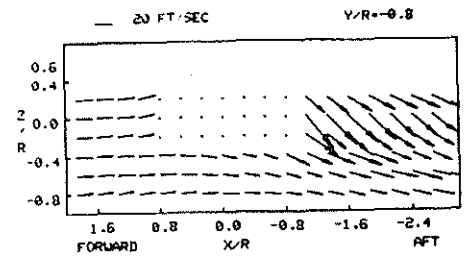

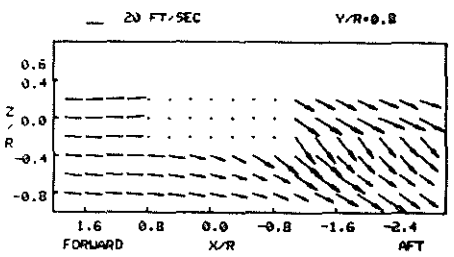

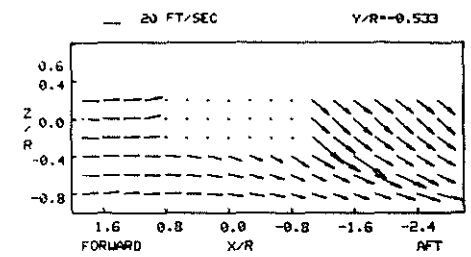

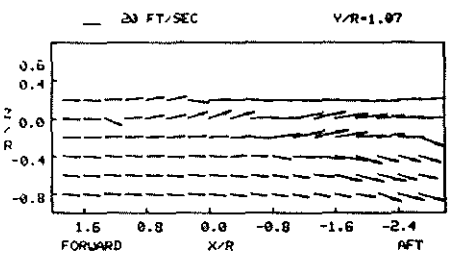

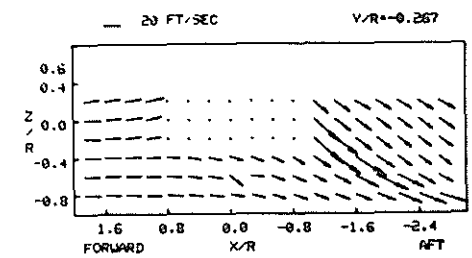

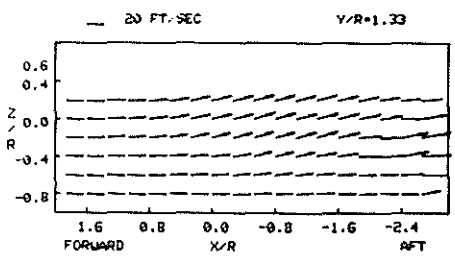

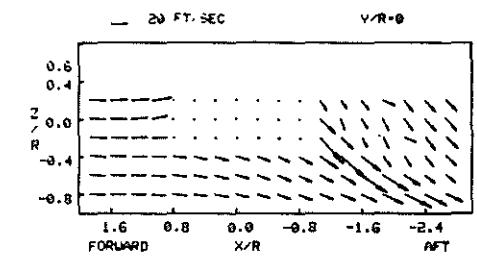

Figure 11.

Velocity vectors in X-Z plane for μ=0.06, θ=8°, and i=2°. Note that coordinates depict probe position only.

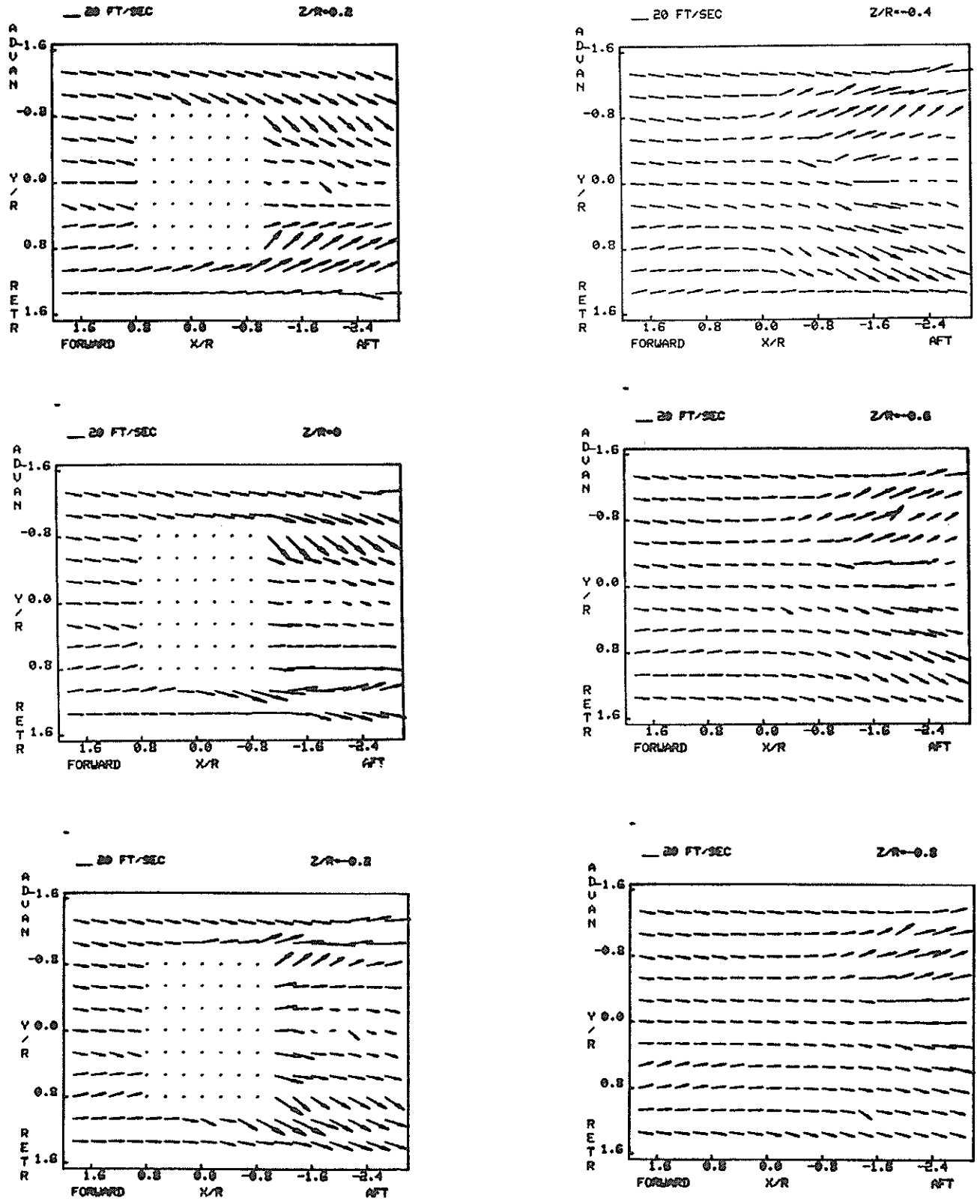

Figure 12.

Velocity vectors in X-Y plane for μ=0.06, θ=8°, and i=2°. Note that coordinates depict probe position only.

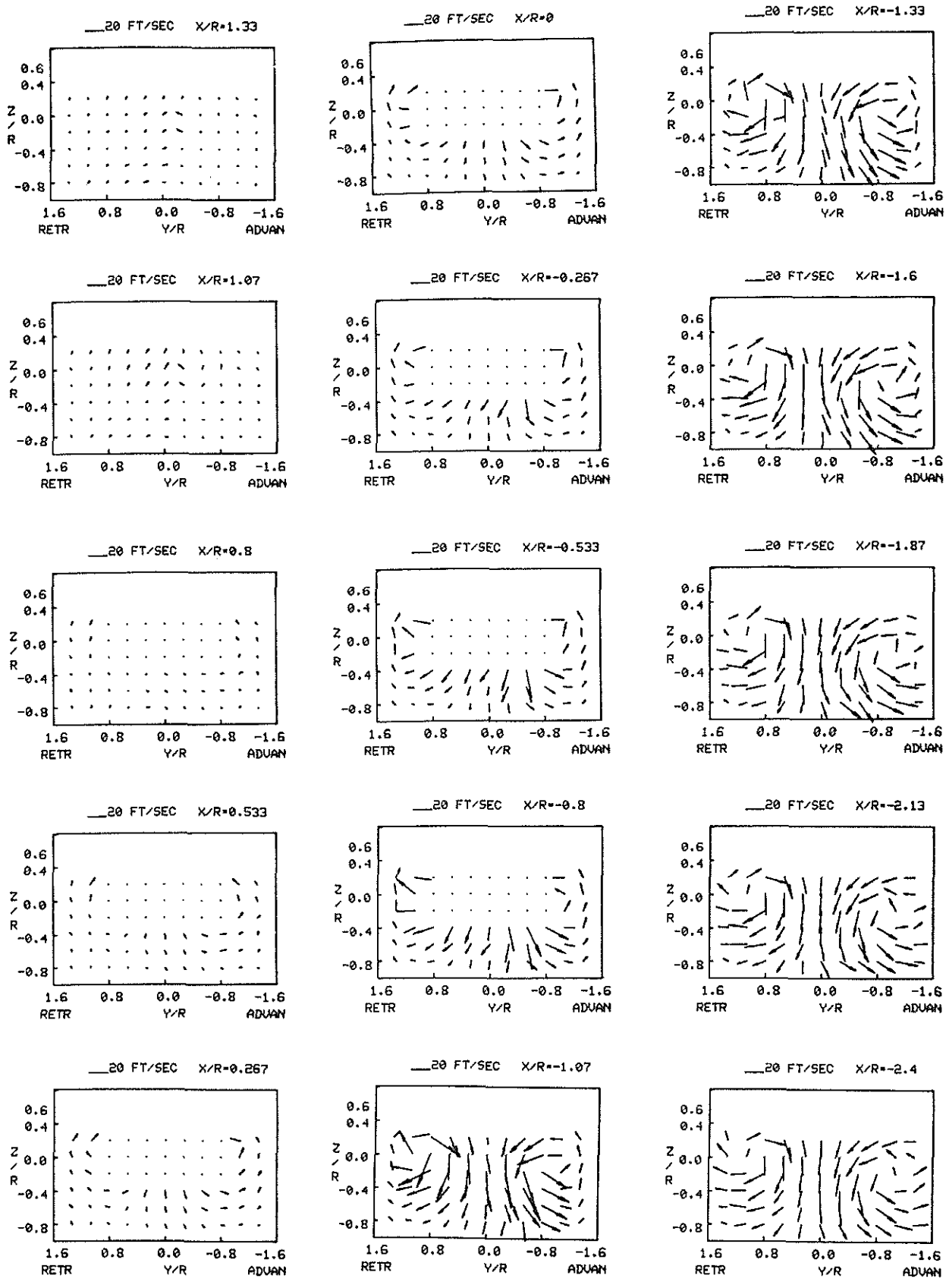

Figure 13.

Velocity vectors in Y-Z plane for μ=0.06, $\theta_{75\%R}$ = 8°, and i=8°. Note that coordinates depict probe position only.

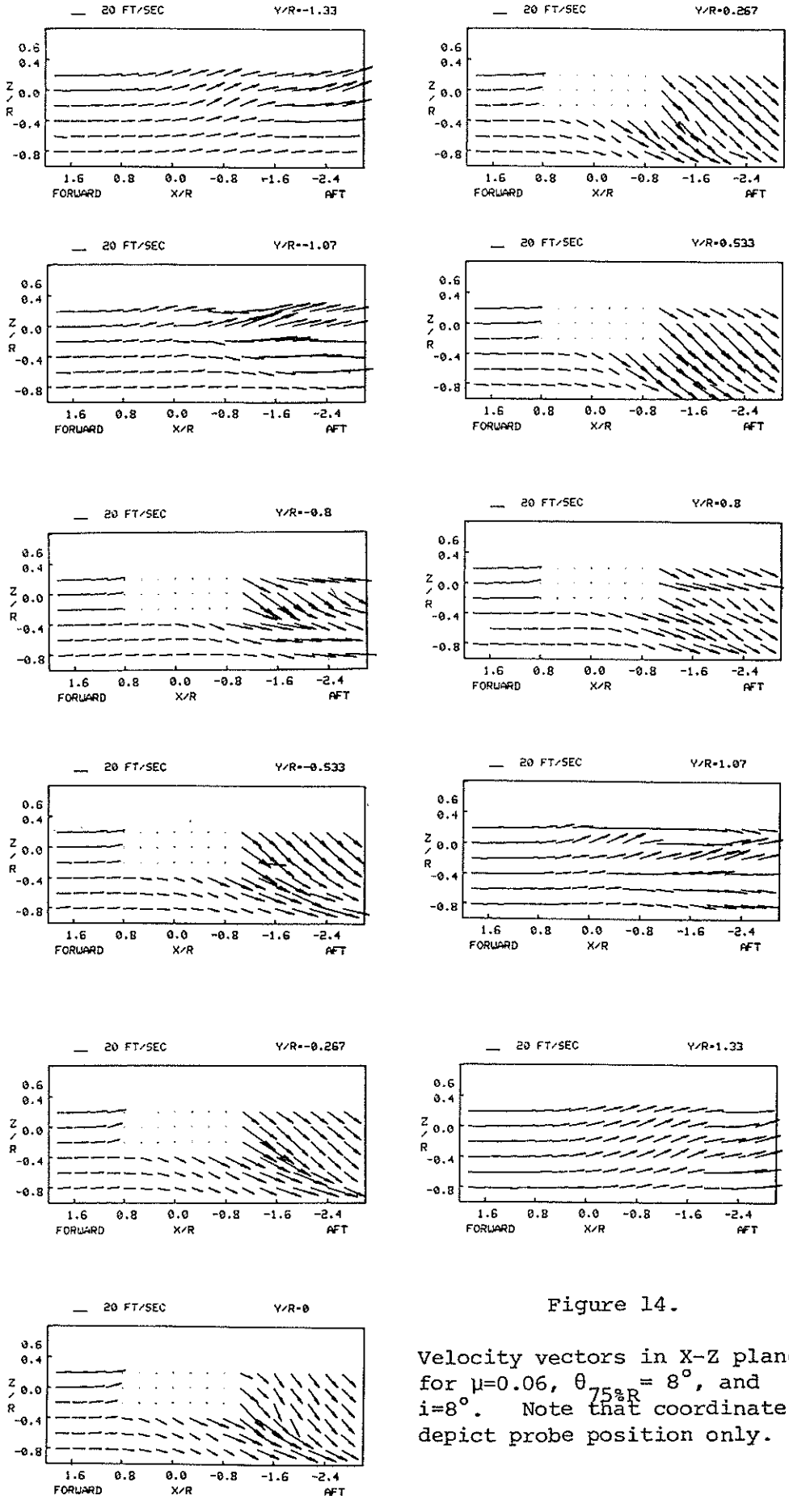

Figure 14.

Velocity vectors in X-Z plane for μ=0.06, $\theta_{75\%R}$ = 8°, and i=8°. Note that coordinates depict probe position only.

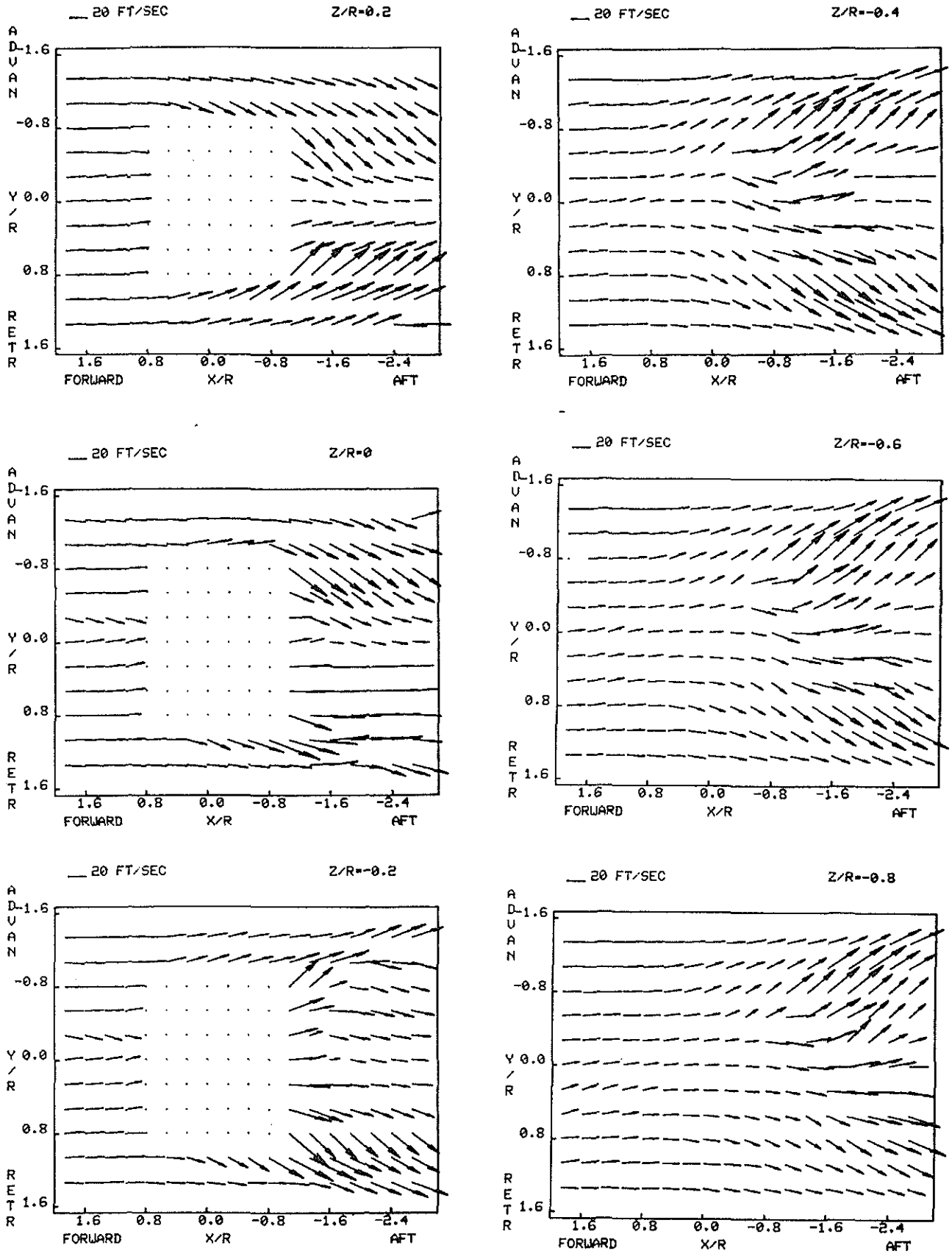

Figure 15.

Velocity vectors in X-Y plane for μ=0.06, $\theta_{75\%R}$, = 8°, and i=8°. Note that coordinates depict probe position only.